Published in final edited form as:
Mol Cancer Ther. 2008 March ; 7(3): 712–720.

Blockade of Viral Interleukin 6 Expression of Kaposi's Sarcoma-Associated Herpesvirus

Yan-Jin Zhang[1,*], **Rheba S. Bonaparte**[1,†], **Deendayal Patel**[1], **David A. Stein**[2], and **Patrick L. Iversen**[2]

1*Molecular Virology Laboratory VA-MD Regional College of Veterinary Medicine University of Maryland College Park, MD 20742*

2*AVI BioPharma Inc. Corvallis, OR 97333*

Abstract

Kaposi's sarcoma-associated herpesvirus (KSHV), also known as human herpesvirus 8, is associated with several malignant disorders, including Kaposi's sarcoma, primary effusion lymphoma (PEL) and multicentric Castleman's disease. An early lytic gene of KSHV encodes vIL-6, a viral homolog of the pro-inflammatory cytokine and an autocrine/paracrine growth factor human interleukin 6. In this study, we examined the effects of suppressing vIL-6 expression in PEL cells with antisense peptide-conjugated phosphorodiamidate morpholino oligomers (PPMO). PPMO are single-stranded DNA analogues that have a modified backbone and enter cells readily. Treatment of PEL cells with a PPMO designed against vIL-6 mRNA led to a marked reduction in the proportion of vIL-6-positive cells detected by immunofluorescence assay. Analysis by Western blot confirmed a specific reduction in the vIL-6 protein level, and demonstrated that the reduction was dependent on the dose of vIL-6 PPMO. PEL cells treated with the vIL-6 PPMO exhibited reduced levels of cellular growth, IL-6 expression and KSHV DNA, as well as an elevated level of p21 protein. Treatment of PEL cells with a combination of two vIL-6 PPMO compounds targeting different sequences in the vIL-6 mRNA led to an inhibitory effect that was greater than that achieved with either PPMO alone. These results demonstrate that PPMO targeting vIL-6 mRNA can potently reduce vIL-6 protein translation, and indicate that further exploration of these compounds in an animal model for potential clinical application is warranted.

Keywords

KSHV; vIL-6; PPMO; Antisense

INTRODUCTION

Kaposi's sarcoma-associated herpesvirus (KSHV) is a member of the gamma herpesviruses and is closely related to Herpesvirus Saimiri (HVS) and Epstein-Barr virus (EBV) (1). KSHV is a double-stranded DNA virus encoding over 80 genes (2). The KSHV gene product vIL-6 has been implicated in the pathogenesis of KSHV-associated lymphoproliferative disorders, such as Primary Effusion Lymphoma (PEL) and Multicentric Castleman's Disease (MCD) (3,4). PEL is a type of B-cell lymphoma known to invade the pleural, pericardial, and peritoneal cavities (5). MCD is characterized by multi-systemic lesions and adenopathy (6). Although the

*Request for reprints: Yan-Jin Zhang, Molecular Virology Laboratory, VA-MD Regional College of Veterinary Medicine, University of Maryland, 8075 Greenmead Drive, College Park, MD 20742. Phone: +1 301 314−6596. Fax: +1 301 314−6855. E-mail address: zhangyj@umd.edu.
†Present address: 7 East 36th Street, Richmond, VA 23224

use of highly active anti-retroviral therapy (HAART) has resulted in a reduced incidence of Kaposi's sarcoma (KS) in industrialized countries, it remains one of the most common malignancies in patients with AIDS (7). Current anti-herpesvirus drugs such as ganciclovir, cidofovir, and foscarnet offer little benefit against either KS and PEL (8,9) because these drugs target KSHV lytic replication, while most tumor cells are latently infected. Thus, drugs effective against KSHV in its latent stage, as well as its lytic stage, may offer significant benefits for the treatment of KSHV-associated malignancies.

KSHV ORF-K2 encodes vIL-6, a homolog of human IL-6 (hIL-6) (3,4). hIL-6 is an important autocrine/paracrine growth factor and is expressed at a relatively high level in some types of lymphoma and leukemia (10-12). Typically, vIL-6 is expressed in only a few cells of KS lesions, but in a greater number of cells in PEL and MCD lesions, indicating a role of vIL-6 in the KSHV-associated lymphoproliferative disorders (13-16). hIL-6 and vIL-6 exhibit differences in receptor usage, with hIL-6 having an absolute requirement for both the gp80 and gp130 subunits of the IL-6 receptor, while vIL-6 apparently requires only gp130 (17). Nevertheless vIL-6 can stimulate all of the known IL-6-induced signaling pathways (17,18) and has been shown to induce the expression of hIL-6 (19). Studies *in vitro* and *in vivo* have shown that vIL-6 can stimulate the growth of KSHV-infected lymphoma cells, promote hematopoiesis, and act as an angiogenic factor through the induction of VEGF (20-23). Intracellular retention and neutralization of vIL-6 with a single-chain antibody inhibited vIL-6-mediated growth of PEL cells and blocked STAT3 phosphorylation in the human hepatoma cell line HepG2 (24). Thus, vIL-6 is a multifunctional cytokine that likely contributes to KSHV-associated lymphoproliferative disorders. Two distinct non-spliced vIL-6 mRNA of 0.95 and 1.1 kb are produced in KSHV-infected PEL cells (25). Two forms of vIL-6 mRNA are transcribed; one initiates at nucleotide (nt) 17980 and the other at nt 18128. Both transcripts end at nt 17182 of the KSHV genome (2).

Phoshorodiamidate morpholino oligomers (PMO) are single-stranded DNA analogs that contain a backbone of morpholine rings and phosphorodiamidate linkages (26). PMO bind to complementary target mRNA by Watson–Crick base pairing and exert an antisense effect by preventing access to critical segments of RNA sequence, such as a translation initiation site, through steric blockade. This is a distinctly different process than the RNase H-dependent mechanism induced by antisense based on DNA chemistry, such as phosphorothioate DNA (26). It has been shown that PMO conjugated to short arginine-rich peptides have a significantly higher efficiency of delivery into cells in culture than do non-conjugated PMO (27). Peptide-conjugated PMO (PPMO) was found to be fairly stable in human serum for at least 24 h (28). Sequence-specific antiviral efficacy of PPMO has been documented against a number of viruses in cell cultures (29-35), and in murine models against Ebola Virus (36), Coxsackievirus B3 (37), murine Coronavirus (38), and West Nile virus (39). In this study, we explored the effects of blocking vIL-6 expression with PPMO in KSHV-infected PEL cells.

In a previous study (33), we documented the efficacy of PPMO designed against mRNA coding for KSHV replication and transcription activator (RTA) and latency-associated nuclear antigen (LANA). An RTA PPMO suppressed RTA protein expression and downstream KSHV proteins in a dose-dependent and sequence-specific manner. KSHV lytic replication was also inhibited. Treatment of BCBL-1 cells with LANA PPMO resulted in a reduction of LANA expression. Considering the important role of vIL-6 in KSHV replication, we sought to explore PPMO technology as a means to reduce vIL-6 expression, with an eye towards development of a therapeutic strategy to treat KSHV-associated malignant diseases.

In the present study, we evaluated four PPMO targeting various regions of vIL-6 transcripts and found that three of the four effectively inhibited vIL-6 expression, as evaluated by immunofluorescence assay and Western blotting. The inhibition of vIL-6 expression in turn

led to reductions of hIL-6 level and KSHV yield in BCBL-1 cells, and to the growth rate of BCBL-1 cells, as well as to an up-regulation of p21 expression.

MATERIALS AND METHODS

Cells and viruses

KSHV-infected cells BC-1 (EBV-positive) and BCBL-1 (EBV-negative) were derived from body cavity-based lymphomas (40,41). BJAB is a KSHV-and EBV-negative lymphoma cell line (42). All cell lines were maintained in RPMI 1640 medium supplemented with 10% fetal bovine serum. For induction of KSHV lytic replication, TPA (12-O-tetratdecanoylphorbol 13-acetate) (Sigma, St Louis, MO) was added to the cell growth medium to a final concentration of 20 ng/mL.

PPMO design and synthesis

PMO were produced at AVI BioPharma Inc. (Corvallis, OR) as previously described (43). Each PMO was covalently conjugated at the 5' end to one of the peptides, NH_2-$R_5F_2R_4C$-$CONH_2$ or NH_2-$(RXR)_4XB$-COOH (where R = arginine, F = phenylalanine, C = cysteine, X = 6-aminohexanoic acid, and B = β-alanine) (abbreviated P4 and P7, respectively), to make PPMO. The conjugation, purification, and analysis of PPMO compounds were similar to methods described elsewhere (27,44). PPMO were designed to be complementary to specific KSHV vIL-6 RNA sequences.

The PPMO sequences used in this study and their target sites are defined in Table 1 and depicted in Figure 1. A random sequence PPMO (named 'CP1'), having little agreement with KSHV or human mRNA sequences, was conjugated to either P4 or P7 peptide and used as negative control PPMO.

PPMO treatment of KSHV-infected PEL cells

Treatment of KSHV-infected BC-1 and BCBL-1 cells was conducted as reported previously (33). Briefly, the cells were pelleted and resuspended in RPMI 1640 medium supplemented with 100 μg/mL BSA, and plated in a 12-well cell culture plate. PPMO was immediately added, mixed, and incubated for 4 h at 37°C. Growth medium was then added to a final volume of 1.5 mL per well. For those cells to be induced with TPA, the medium was supplemented with TPA at 20 ng/mL. The cells were incubated for 48 h at 37°C and both cells and culture supernatants then harvested for further analysis.

Immunofluorescence assay (IFA)

IFA was utilized to detect KSHV proteins in cells as described previously (33). Briefly, cells were pelleted, rinsed in PBS three times, and spotted onto Teflon-coated slides. The slides were air dried, fixed with 1% paraformaldehyde for 10 minutes, and treated with 0.5% Triton X-100 for 5 minutes at room temperature. Rabbit anti-vIL-6 antibody (Advanced Biotechnologies Inc., Columbia, MD) was used to detect vIL-6 expression in PEL cells. Goat anti-rabbit IgGFITC (Sigma) conjugate was used to identify specific reactions between primary antibody and target protein. The stained cells were observed under fluorescence microscopy.

Western blot analysis

Expression of vIL-6 protein in KSHV-infected cells was detected by Western blot. BCBL-1 cells were lysed and resolved in 12% polyacrylamide gels by SDS-PAGE. The separated proteins were transferred to nitrocellulose membrane, probed with rabbit anti-vIL-6 antibody and goat anti-rabbit IgG conjugated with horseradish peroxidase (Sigma), and revealed with the addition of chemiluminescence substrate. Chemiluminescence signals were collected in

ChemiDoc digital imaging system (Bio-Rad Laboratories, Hercules, CA). Beta-tubulin was detected on the same blot membrane to normalize the protein loading in the blot analysis. Similarly, p21 protein in PEL cells was detected with mouse anti-p21 monoclonal antibody (Invitrogen, Carlsbad, CA). Digital image analyses were conducted using Quantity One software (Version 4.4) (Bio-Rad).

Detection of hIL-6 in BCBL-1 culture supernatant

PPMO was added to BCBL-1 cells and culture supernatant was harvested 48 h later. IL-6 level in the supernatant was analyzed by IL-6 EIA kit (Assay Designs, Ann Arbor, Michigan) to assess hIL-6 expression under the different treatment conditions. Standard curve of IL-6 concentration was generated with IL-6 supplied in the kit per manufacturer's instructions. BCBL-1 cells with or without TPA induction were included as controls.

Cell viability assay

The viability of BCBL-1 cells after PPMO- or mock-treatment was determined with CellTiter-Glo® Luminescent Cell Viability Assay (Promega, Madison, WI). Briefly, BCBL-1 cells were treated with ILP1 or CP1 and cultured for 24 h. No TPA was included in the culture medium. CellTiter-Glo reagent was added and incubated for 10 min at room temperature. The luminescence signal was measured with a VICTOR3™ Multilabel Counter (PerkinElmer Life and Analytical Sciences, Wellesley, MA). Relative percentages of luminescence intensity were calculated by comparison to mock-treated controls.

Statistical analysis

A single factor ANOVA statistical analysis was conducted to test differences between the treatment groups. A two-tailed P value of less than 0.05 was considered to be a significant difference.

DNA isolation and real-time PCR

Genomic DNA from cell culture supernatant was isolated using DNAzol (Invitrogen) and DNA from cells with Wizard Genomic DNA Purification Kit (Promega). Real-time PCR was conducted with a Chromo 4 Detector system (Bio-Rad) using a primer set (73-RF2, 5’ TGACT TCGCC AACCG TAG 3’ and 73-RR2, 5’ CCTAT GGAGA TGGGA GATGT AG 3’) that was expected to amplify sequence in the ORF73 gene, and iQ SYBR Green Supermix (Bio-Rad). A recombinant plasmid pcDNA3.1/His-ORF73 was quantified and used to generate standard curves for the real-time PCR. DNA of β-actin was also amplified from the cellular DNA in order to assure normalized quantitative PCR detection of KSHV DNA from cells.

RESULTS

Design of PPMO against KSHV vIL-6 transcripts

A 21mer PPMO (ILP1) complementary in sequence to the ORF-K2 translation initiation region (Table 1 and Fig. 1) was prepared for use in initial cell-culture studies as a P4-PMO. Two transcripts of different lengths encoding vIL-6 have been found in KSHV-infected PEL cells (25). These two transcripts have the same 3’ terminus but different 5’ transcription start sites, leading to 148 nucleotides difference in the length of 5’ untranslated region (UTR). PPMO ILP2, ILP3, and ILP4 were were prepared as P7-PMO and designed to target various other sites in the 5’UTR of the vIL-6 transcripts (Fig. 1), with the intention of further exploring PPMO-mediated inhibition of vIL-6 expression. Specifically, ILP2, a 23mer, is contiguously complementary to the 17 nucleotides at the 5’-terminus of the longer transcript and 6 nucleotides of KSHV DNA immediately upstream of the transcription start site of the longer vIL-6 transcript; ILP3 is complementary to sequence of the longer transcript located

immediately upstream of sequence corresponding to the 5'terminus of the shorter transcript, and ILP4 is complementary to sequence found in the 5'UTR of both the shorter and the longer transcripts..

IFA detection of PPMO-mediated reduction of vIL-6 protein expression in KSHV-infected PEL cells

Initially, ILP1 PPMO was tested for its effect on vIL-6 protein expression. BCBL-1 cells were treated with ILP1 or CP1 at 8 and 16 μM. Growth medium containing TPA was added to BCBL-1 cells to induce KHSV lytic replication. After two-days in culture, a portion of the cells were fixed for IFA to determine the vIL-6 protein expression after PPMO treatment. Another portion was harvested for SDS-PAGE and Western blot analysis. In a separate experiment, ILP2, ILP3, ILP4, and CP1 were used to treat BCBL-1 cells in a similar manner.

Observation by fluorescence microscopy revealed that after TPA induction approximately 16% of BCBL-1 cells expressed vIL-6 (Fig. 1B). In non-induced BCBL-1 cells, approximately 1% of cells were vIL-6-positive, indicating spontaneous KSHV lytic replication was occurring in only a small number of cells, as expected. In TPA-induced cells, treatment with 16 μM ILP1 PPMO resulted in 4% vIL-6-positive cells, compared to 13% for cells treated with 16 μM CP1 PPMO (Fig. 1B). Pursuant to this observation, ILP2, ILP3, and ILP4 were used to treat BCBL-1 cells. Cells treated with ILP2, ILP3, and ILP4 had approximately 10%, 4%, and 3%, respectively, vIL-6-positive cells. The results demonstrated that treatment with ILP1, ILP3, and ILP4, but not ILP2, substantially reduced vIL-6 protein expression.

Western blot detection of PPMO-mediated inhibition of vIL-6 protein expression in PEL cells

Having observed reduction of vIL-6 expression in PPMO-treated BCBL-1 cells by IFA, we conducted Western blot analysis to confirm and further characterize PPMO suppression of vIL-6 protein level in the cells. Total cell lysates were prepared from BCBL-1 cells treated with ILP1 PPMO and subjected to SDS-PAGE and Western blotting with vIL-6 antibody. In comparison with the mock-treated control, treatment of BCBL-1 cells with ILP1 decreased vIL-6 protein expression, while treatment with CP1 resulted in no detectable change (Fig. 2A). Quantitative image analysis revealed that 8 and 16 μM ILP1 PPMO reduced vIL-6 expression by approximately 60% and over 90%, respectively, compared to mock-treated control (Fig 2A). This result confirmed the IFA observation and demonstrated that ILP1 inhibited vIL-6 expression in a sequence-dependent manner.

Samples from cells treated with PPMO ILP2, ILP3, and ILP4 were also evaluated for reduction of vIL-6 protein level. Western blot analysis showed that ILP3 and ILP4 treatment reduced vIL-6 protein expression, while ILP2 had no inhibitory effect (Fig. 2B). Quantitative image analysis revealed that treatment of BCBL-1 cells with ILP3 and ILP4 at 16 μM led to reduction of vIL-6 protein level by 79% and 99%, respectively, compared to mock-treated control (Fig. 2B).

Inhibition of vIL-6 expression by PPMO in BC-1 cells. PEL cells can be infected by both KSHV and EBV. To assess the inhibitory effect of PPMO on vIL-6 expression in such PEL cells, we conducted PPMO treatment of BC-1 cells in the same manner as that described above for BCBL-1 cells. IFA showed that after TPA induction and ILP1 treatment, the number of vIL-6-positive BC-1 cells was markedly reduced (data not shown).

Western blot analysis confirmed that treatment of BC-1 cells with ILP1 resulted in reduced vIL-6 protein expression, while CP1-treated cells had a similar vIL-6 level to that of the mock-treated control (Fig 2C). Quantitative image analysis revealed that treatment of BC-1 cells with 8 and 16 μM ILP1 led to 77% and 85% reduction of vIL-6 protein level, compared with the

mock-treated control (Fig. 2C). This result demonstrates that ILP1 is effective at inhibiting vIL-6 protein expression in BC-1 cells and that the effectiveness of this PPMO is not cell-line specific.

Combinatory effect of PPMO against vIL-6. To determine whether combination of two PPMO compounds against vIL-6 would yield significantly higher inhibition than either PPMO alone, we tested treatment of BCBL-1 cells with ILP3 and ILP4, individually and together. Western blot analysis and quantitative image analysis of the blot (Fig. 2D) show that a combination treatment with ILP3 and ILP4, each present at 2 μM (lane 9), led to a significantly lower level of vIL-6 protein than either PPMO alone at 2 μM (compare lane 9 with lane 3 or 6). Treatment with 4 μM ILP4 resulted in a far lower level of vIL-6 expression than did treatment with 4 μM ILP3. Together, the results suggest that a combination of ILP3 and ILP4 PPMO compounds produced an enhanced inhibition of vIL-6 expression in BCBL-1 cells.

These results indicate that ILP1, ILP3, and ILP4 inhibited vIL-6 protein expression in BCBL-1 cells in a sequence-specific manner. Since these three PPMO produced a similar level of inhibitory effect on vIL-6 protein expression, and the ILP1 PPMO contained the same peptide as those PPMO used in our previous study (33), we chose ILP1 to conduct further analysis of the effects of vIL-6 PPMO on KHSV-infected PEL cells.

PPMO effect on hIL-6 expression

Since vIL-6 is both a structural and functional homolog of hIL-6, and the presence of vIL-6 has been shown to up-regulate the expression of hIL-6 (19), we sought to determine if suppression of vIL-6 could lead to a reduction of hIL-6 expression. As hIL-6 is a secreted cytokine, supernatants from each well of PPMO-treated BCBL-1 cells were analyzed with an IL-6 EIA kit (Assay Designs).

After TPA induction in BCBL-1 cells, hIL-6 expression was elevated approximately 6-fold (Fig. 3A), as expected. Treatment of the cells with 16 μM ILP1 led to ~2-fold reduction of hIL-6, while the cells treated with CP1 exhibited similar level of hIL-6 as the TPA-induction control. Thus, ILP1-mediated inhibition of vIL-6 in BCBL-1 cells resulted in a substantial reduction of hIL-6 expression.

Reduction of growth of BCBL-1 cells

IL-6 is thought to play an important role in the growth of KSHV-infected PEL cells. Intracellular retention of single chain anti-vIL-6 antibody in BCBL-1 cells inhibited growth (24). Since vIL-6 expression was inhibited by vIL-6 PPMO, we sought to test whether ILP1 treatment could result in inhibition of growth of PEL cells. BCBL-1 cells were treated with ILP1, with no TPA induction. BJAB cells were treated in the same manner and included as a control. At 24 h after PPMO treatment, a cell-viability assay was conducted. Treatment of BCBL-1 cells with 8 μM ILP1 led to an approximately 2-fold reduction of cell growth (Fig. 3B). The application of ILP1 or CP1 to BJAB cells did not have an observable effect on cell growth (Fig. 3C).

Elevation of p21 level in PPMO-treated BCBL-1 cells

Since treatment of BCBL-1 cells with ILP1 led to reduction of cell growth, and p21 is a cyclin-dependent kinase inhibitor in cell cycle regulation, we sought to evaluate the effect of ILP1 treatment on p21 protein expression. Western blotting demonstrated that p21 level in BCBL-1 cells after ILP1 treatment was elevated (Fig. 4). Quantitative image analysis showed that the p21 protein level in cells treated with ILP1 was 13-fold higher than that in the mock-treated control. The result indicates that ILP1 treatment led to an up-regulation of p21 expression, which we assume could have an impact on cell growth.

PPMO effect on KSHV replication

As an early lytic gene, vIL-6 likely plays an important role in maintaining PEL cell growth. Therefore, suppression of vIL-6 expression could be expected to have an effect on KSHV lytic replication. To test this speculation, BCBL-1 cells were treated with ILP1 and CP1 and treated with TPA to induce KSHV lytic replication. Cell culture supernatant and cells were harvested for DNA isolation. Cells without TPA induction were included for comparison. To measure KSHV DNA level, real-time PCR was conducted with DNA from intracellular and cell culture supernatant samples. In this experiment, TPA induction led to an elevation of KSHV viral DNA level by 3.0- and 3.3-fold in cells and culture supernatants, respectively (Fig. 5). Cells treated with CP1 had a viral DNA level similar to the background level observed in the mock-treated samples. The intracellular and supernatant levels of KSHV DNA from cells treated with ILP1 at 16 μM was 2.2- and 2.1-fold lower, respectively, than those of mock-treated controls (Fig. 5). The result indicates treatment with ILP1 resulted in reduction of KSHV replication in BCBL-1 cells.

DISCUSSION

In this study, we show that vIL-6 PPMO treatment inhibited vIL-6 protein expression in two lines of KSHV-infected PEL cells, BCBL-1 and BC-1. In addition, the antisense-mediated inhibition of vIL-6 expression was sequence-specific, as both the control PPMO CP1 and the ILP2 PPMO had minimal effect.

Two species of vIL-6 transcript are produced in BCBL-1 cells, with one transcript 148 nucleotides longer in the 5'UTR than the other (25). PPMO were designed to complement the two types of transcripts at different target sites. ILP1 and ILP4 are fully complementary to both species of transcripts and were shown to be effective inhibitors of vIL-6 expression. ILP3 complements only the longer vIL-6 transcript, suggesting that the vIL-6 protein in ILP3-treated cells was produced at least partially from translation of the shorter vIL-6 transcript. These results suggest that both vIL-6 transcripts are translated in TPA-induced BCBL-1 cells. However, the possibility that ILP1 and ILP4 are simply more effective than ILP3 at blocking translation of the longer mRNA transcript cannot be excluded.

IL-6 is believed to be an important growth factor in KSHV-infected PEL cells (12,45). Apparently as a result of vIL-6 reduction, the hIL-6 level in BCBL-1 cells was decreased (Fig. 3A). Pursuant to this finding, we further conducted cell growth assays in the presence and absence of ILP1 PPMO. The growth assays were done without TPA induction, to avoid any effect from KSHV lytic replication. The growth of BCBL-1 cells was reduced after treatment with ILP1 (Fig. 3B). This result is consistent with a previous report that vIL-6 induces the expression of hIL-6 (19). Further, it indicates that even if it is expressed in less than 5% of the cells, vIL-6 plays a role in maintaining BCBL-1 cell growth, suggesting a paracrine mechanism for its activity. The result here showing BCBL-1 growth inhibition by vIL-6 PPMO is consistent with a previous finding that intracellular retention and neutralization of vIL-6 by a single-chain anti-vIL-6 antibody inhibited BCBL-1 cell growth (24).

It was previously reported that clonal growth of KS-1 and BC-1 cells was inhibited by hIL-6 antisense phosphorothioate oligonucleotides, but not by vIL-6- or IL-10-directed phosphorothioates (45). We obtained different results using PPMO vIL-6 antisense, perhaps because of the different chemistries of the antisense structural types employed, or because the exact vIL-6 target sequences varied between the two studies.

p21 is an important inhibitor of cyclin-dependent kinase, and the upregulation of this protein may have an impact on cell growth. An elevated p21 level may lead to growth arrest. IL-6 is

a growth factor, and its reduction may lead to increased p21 expression. However, our result does not represent a causal link between the relative expression of IL-6 and p21 proteins.

In PEL cells, TPA induction activates KSHV lytic replication (41). Due to the important role of vIL-6 in BCBL-1 growth, we speculated that vIL-6 blockade may have a negative consequence for KSHV replication. Using real-time PCR, we found that both intracellular and extra-cellular KSHV DNA yield in BCBL-1 cells was reduced after ILP1 treatment. Since the expression of vIL-6 is downstream of RTA, an immediate early gene in KSHV lytic replication, vIL-6 blockade may not have a direct effect on the KSHV lytic cascade. In addition, protein expression of KSHV RTA, vIRF-1, K8.1A, and LANA were not affected by a reduction of vIL-6 protein expression (data not shown).

Our earlier study showed that PPMO can specifically suppress protein expression of KSHV RTA and LANA (33). Application of RTA-specific PPMO to BCBL-1 cells resulted in inhibition of KSHV viral DNA levels in intracellular and culture supernatant samples. In the present study, we observed that vIL-6 PPMO treatment produced effective inhibition of vIL-6 protein expression and that treatment with the vIL-6 PPMO produced a higher inhibition of vIL-6 protein production than that of RTA PPMO treatment (data not shown). This observation indicates that, not surprisingly, directly targeting vIL-6 transcripts with PPMO produces more effective inhibition than blocking expression of an upstream gene.

Current anti-herpesvirus drugs target the lytic rather than the latent phase of herpesvirus replication, and it has been reported that cidofovir and foscarnet are the most efficient commercially available compounds against KSHV (46-48). Cidofovir and foscarnet have no effect on expression of latent or early lytic genes (49), as these drugs are inhibitors of the viral DNA polymerase, and transcription of early lytic genes occurs before DNA replication in KSHV. Early lytic genes such as vIL-6 play important roles in KSHV replication and pathogenesis (16,20,21). Blocking expression of these genes could contribute to the treatment of KSHV-associated malignancies. Our results indicate that vIL-6 may be an effective target for controlling PEL cell growth, which may have positive implications for managing KSHV-induced lymphoma development. Further studies to investigate the capacity of PPMO compounds to block lymphoma development in a SCID mouse model of PEL are warranted.

ACKNOWLEDGEMENT

We gratefully acknowledge the Chemistry Department of AVI BioPharma Inc. for the synthesis and quality control of all PPMO compounds used in this study. BCBL-1 cells were obtained through the NIH AIDS Research and reference Reagent Program, Division of AIDS, NIAID, NIH (Cat# 3233, originally from Drs. Michael McGrath and Don Ganem). This work was supported by Public Health Service grant CA-103612 to Y. Zhang from the National Cancer Institute, NIH.

Abbreviation list

KSHV, Kaposi's sarcoma-associated herpesvirus; PEL, primary effusion lymphoma; PMO, phosphorodiamidate morpholino oligonucleotides; PPMO, peptide-conjugated PMO; vIL-6, viral homolog of human IL-6; RTA, replication and transcription activator; LANA, latency-associated nuclear antigen; ILP1, PPMO 1 against vIL-6; CP1, control PMO..

REFERENCES

1. Chang Y, Cesarman E, Pessin MS, et al. Identification of herpesvirus-like DNA sequences in AIDS-associated Kaposi's sarcoma. Science 1994;266:1865–9. [PubMed: 7997879]
2. Russo JJ, Bohenzky RA, Chien MC, et al. Nucleotide sequence of the Kaposi sarcoma-associated herpesvirus (HHV8). Proc Natl Acad Sci USA 1996;93:14862–7. [PubMed: 8962146]

3. Moore PS, Boshoff C, Weiss RA, Chang Y. Molecular mimicry of human cytokine and cytokine response pathway genes by KSHV. Science 1996;274:1739–44. [PubMed: 8939871]
4. Nicholas J, Ruvolo VR, Burns WH, et al. Kaposi's sarcoma-associated human herpesvirus-8 encodes homologues of macrophage inflammatory protein-1 and interleukin-6. Nat Med 1997;3:287–92. [PubMed: 9055855]
5. Jaffe E. Primary body cavity-based AIDS-related lymphomas. Evolution of a new disease entity. Am J Clin Pathol 1996;105:221–9. [PubMed: 8607449]
6. Soulier J, Grollet L, Oksenhendler E, et al. Molecular analysis of clonality in Castleman's disease. Blood 1995;86:1131–8. [PubMed: 7620166]
7. Engels EA, Pfeiffer RM, Goedert JJ, et al. Trends in cancer risk among people with AIDS in the United States 1980−2002. AIDS 2006;20:1645–54. [PubMed: 16868446]
8. Robles R, Lugo D, Gee L, Jacobson MA. Effect of antiviral drugs used to treat cytomegalovirus end-organ disease on subsequent course of previously diagnosed Kaposi's sarcoma in patients with AIDS. J Acquir Immune Defic Syndr Hum Retrovirol 1999;20:34–8. [PubMed: 9928727]
9. Little RF, Merced-Galindez F, Staskus K, et al. A pilot study of cidofovir in patients with kaposi sarcoma. J Infect Dis 2003;187:149–53. [PubMed: 12508160]
10. Bataille R, Harousseau JL. Multiple myeloma. N Engl J Med 1997;336:1657–64. [PubMed: 9171069]
11. Yoshizaki K, Matsuda T, Nishimoto N, et al. Pathogenic significance of interleukin-6 (IL-6/BSF-2) in Castleman's disease. Blood 1989;74:1360–7. [PubMed: 2788466]
12. Miles SA, Rezai AR, Salazar-Gonzalez JF, et al. AIDS Kaposi sarcoma-derived cells produce and respond to interleukin 6. Proc Natl Acad Sci USA 1990;87:4068–72. [PubMed: 1693429]
13. Parravinci C, Corbellino M, Paulli M, et al. Expression of a virus-derived cytokine, KSHV vIL-6, in HIV-seronegative Castleman's disease. Am J Pathol 1997;151:1517–22. [PubMed: 9403701]
14. Sun R, Lin SF, Staskus K, et al. Kinetics of Kaposi's sarcoma-associated herpesvirus gene expression. J Virol 1999;73:2232–42. [PubMed: 9971806]
15. Cannon JS, Nicholas J, Orenstein JM, et al. Heterogeneity of viral IL-6 expression in HHV-8-associated diseases. J Infect Dis 1999;180:824–8. [PubMed: 10438372]
16. Staskus KA, Sun R, Miller G, et al. Cellular tropism and viral interleukin-6 expression distinguish human herpesvirus 8 involvement in Kaposi's sarcoma, primary effusion lymphoma, and multicentric Castleman's disease. J Virol 1999;73:4181–7. [PubMed: 10196314]
17. Molden J, Chang Y, You Y, Moore PS, Goldsmith MA. A Kaposi's sarcoma-associated herpesvirus-encoded cytokine homolog (vIL- 6) activates signaling through the shared gp130 receptor subunit. J Biol Chem 1997;272:19625–31. [PubMed: 9235971]
18. Osborne J, Moore PS, Chang Y. KSHV-encoded viral IL-6 activates multiple human IL-6 signaling pathways. Hum Immunol 1999;60:921–7. [PubMed: 10566591]
19. Mori Y, Nishimoto N, Ohno M, et al. Human herpesvirus 8-encoded interleukin-6 homologue (viral IL-6) induces endogenous human IL-6 secretion. J Med Virol 2000;61:332–5. [PubMed: 10861641]
20. Aoki Y, Jaffe ES, Chang Y, et al. Angiogenesis and hematopoiesis induced by Kaposi's sarcoma-associated herpesvirus-encoded interleukin-6. Blood 1999;93:4034–43. [PubMed: 10361100]
21. Jones KD, Aoki Y, Chang Y, Moore PS, Yarchoan R, Tosato G. Involvement of interleukin-10 (IL-10) and viral IL-6 in the spontaneous growth of Kaposi's sarcoma herpesvirus-associated infected primary effusion lymphoma cells. Blood 1999;94:2871–9. [PubMed: 10515891]
22. Klouche M, Brockmeyer N, Knabbe C, Rose-John S. Human herpesvirus 8-derived viral IL-6 induces PTX3 expression in Kaposi's sarcoma cells. AIDS 2002;16:F9–18. [PubMed: 12004288]
23. Chatterjee M, Osborne J, Bestetti G, Chang Y, Moore PS. Viral IL-6-induced cell proliferation and immune evasion of interferon activity. Science 2002;298:1432–5. [PubMed: 12434062]
24. Kovaleva M, Bussmeyer I, Rabe B, et al. Abrogation of viral interleukin-6 (vIL-6)-induced signaling by intracellular retention and neutralization of vIL-6 with an anti-vIL-6 single-chain antibody selected by phage display. J Virol 2006;80:8510–20. [PubMed: 16912301]
25. Deng H, Song MJ, Chu JT, Sun R. Transcriptional regulation of the interleukin-6 gene of human herpesvirus 8 (Kaposi's sarcoma-associated herpesvirus). J Virol 2002;76:8252–64. [PubMed: 12134031]

26. Summerton J. Morpholino antisense oligomers: the case for an RNase H-independent structural type. Biochim Biophys Acta 1999;1489:141–58. [PubMed: 10807004]
27. Moulton HM, Nelson MH, Hatlevig SA, Reddy MT, Iversen PL. Cellular uptake of antisense morpholino oligomers conjugated to arginine-rich peptides. Bioconjug Chem 2004;15:290–9. [PubMed: 15025524]
28. Youngblood DS, Hatlevig SA, Hassinger JN, Iversen PL, Moulton HM. Stability of cell-penetrating Peptide-morpholino oligomer conjugates in human serum and in cells. Bioconjug Chem 2007;18:50–60. [PubMed: 17226957]
29. Kinney RM, Huang CY, Rose BC, et al. Inhibition of Dengue Virus Serotypes 1 to 4 in Vero Cell Cultures with Morpholino Oligomers. J Virol 2005;79:5116–28. [PubMed: 15795296]
30. Neuman BW, Stein DA, Kroeker AD, et al. Inhibition and escape of SARS-CoV treated with antisense morpholino oligomers. Adv Exp Med Biol 2006;581:567–71. [PubMed: 17037599]
31. Zhang YJ, Stein DA, Fan SM, et al. Suppression of porcine reproductive and respiratory syndrome virus replication by morpholino antisense oligomers. Vet Microbiol 2006;117:117–29. [PubMed: 16839712]
32. Deas TS, Binduga-Gajewska I, Tilgner M, et al. Inhibition of Flavivirus Infections by Antisense Oligomers Specifically Suppressing Viral Translation and RNA Replication. J Virol 2005;79:4599–609. [PubMed: 15795246]
33. Zhang YJ, Wang KY, Stein DA, et al. Inhibition of replication and transcription activator and latency-associated nuclear antigen of Kaposi's sarcoma-associated herpesvirus by morpholino oligomers. Antiviral Res 2007;73:12–23. [PubMed: 16842866]
34. Ge Q, Pastey M, Kobasa D, et al. Inhibition of Multiple Subtypes of Influenza A Virus in Cell Cultures with Morpholino Oligomers. Antimicrob Agents Chemother 2006;50:3724–33. [PubMed: 16966399]
35. van den Born E, Stein DA, Iversen PL, Snijder EJ. Antiviral activity of morpholino oligomers designed to block various aspects of Equine arteritis virus amplification in cell culture. J Gen Virol 2005;86:3081–90. [PubMed: 16227231]
36. Enterlein S, Warfield KL, Swenson DL, et al. VP35 Knockdown Inhibits Ebola Virus Amplification and Protects against Lethal Infection in Mice. Antimicrob Agents Chemother 2006;50:984–93. [PubMed: 16495261]
37. Yuan J, Stein DA, Lim T, et al. Inhibition of Coxsackievirus B3 in Cell-cultures and in Mice by Peptide-Conjugated Morpholino Oligomers Targeting the IRES. J Virol 2006;80:11510–9. [PubMed: 16987987]
38. Burrer R, Neuman BW, Ting JP, et al. Antiviral effects of antisense morpholino oligomers in murine coronavirus infection models. J Virol 2007;81:5637–48. [PubMed: 17344287]
39. Deas TS, Bennett CJ, Jones SA, et al. In Vitro Resistance Selection and In Vivo Efficacy of Morpholino Oligomers against West Nile Virus. Antimicrob Agents Chemother 2007;51:2470–82. [PubMed: 17485503]
40. Cesarman E, Moore PS, Rao PH, Inghirami G, Knowles DM, Chang Y. *In vitro* establishment and characterization of two acquired immunodeficiency syndrome-related lymphoma cell lines (BC-1 and BC-2) containing Kaposi's sarcoma-associated herpesvirus-like (KSHV) DNA sequences. Blood 1995;86:2708–14. [PubMed: 7670109]
41. Renne R, Zhong W, Herndier B, et al. Lytic growth of Kaposi's sarcoma-associated herpesvirus (human herpesvirus 8) in culture. Nat Med 1996;2:342–6. [PubMed: 8612236]
42. Menezes J, Leibold W, Klein G, Clements G. Establishment and characterization of an Epstein-Barr virus (EBC)-negative lymphoblastoid B cell line (BJA-B) from an exceptional, EBV-genome-negative African Burkitt's lymphoma. Biomedicine 1975;22:276–84. [PubMed: 179629]
43. Summerton J, Weller D. Morpholino antisense oligomers: design, preparation, and properties. Antisense Nucleic Acid Drug Dev 1997;7:187–95. [PubMed: 9212909]
44. Abes S, Moulton HM, Clair P, et al. Vectorization of morpholino oligomers by the (R-Ahx-R)4 peptide allows efficient splicing correction in the absence of endosomolytic agents. J Control Release 2006;116:304–13. [PubMed: 17097177]
45. Asou H, Said JW, Yang R, et al. Mechanisms of growth control of Kaposi's sarcoma-associated herpes virus-associated primary effusion lymphoma cells. Blood 1998;91:2475–81. [PubMed: 9516148]

46. Kedes DH, Ganem D. Sensitivity of Kaposi's sarcoma-associated herpesvirus replication to antiviral drugs. Implications for potential therapy. J Clin Invest 1997;99:2082–6. [PubMed: 9151779]

47. Medveczky MM, Horvath E, Lund T, Medveczky PG. In vitro antiviral drug sensitivity of the Kaposi's sarcoma-associated herpesvirus. AIDS 1997;11:1327–32. [PubMed: 9302441]

48. Sergerie Y, Boivin G. Evaluation of susceptibility of human herpesvirus 8 to antiviral drugs by quantitative real-time PCR. J Clin Microbiol 2003;41:3897–900. [PubMed: 12904413]

49. Curreli F, Cerimele F, Muralidhar S, et al. Transcriptional downregulation of ORF50/Rta by methotrexate inhibits the switch of Kaposi's sarcoma-associated herpesvirus/human herpesvirus 8 from latency to lytic replication. J Virol 2002;76:5208–19. [PubMed: 11967335]

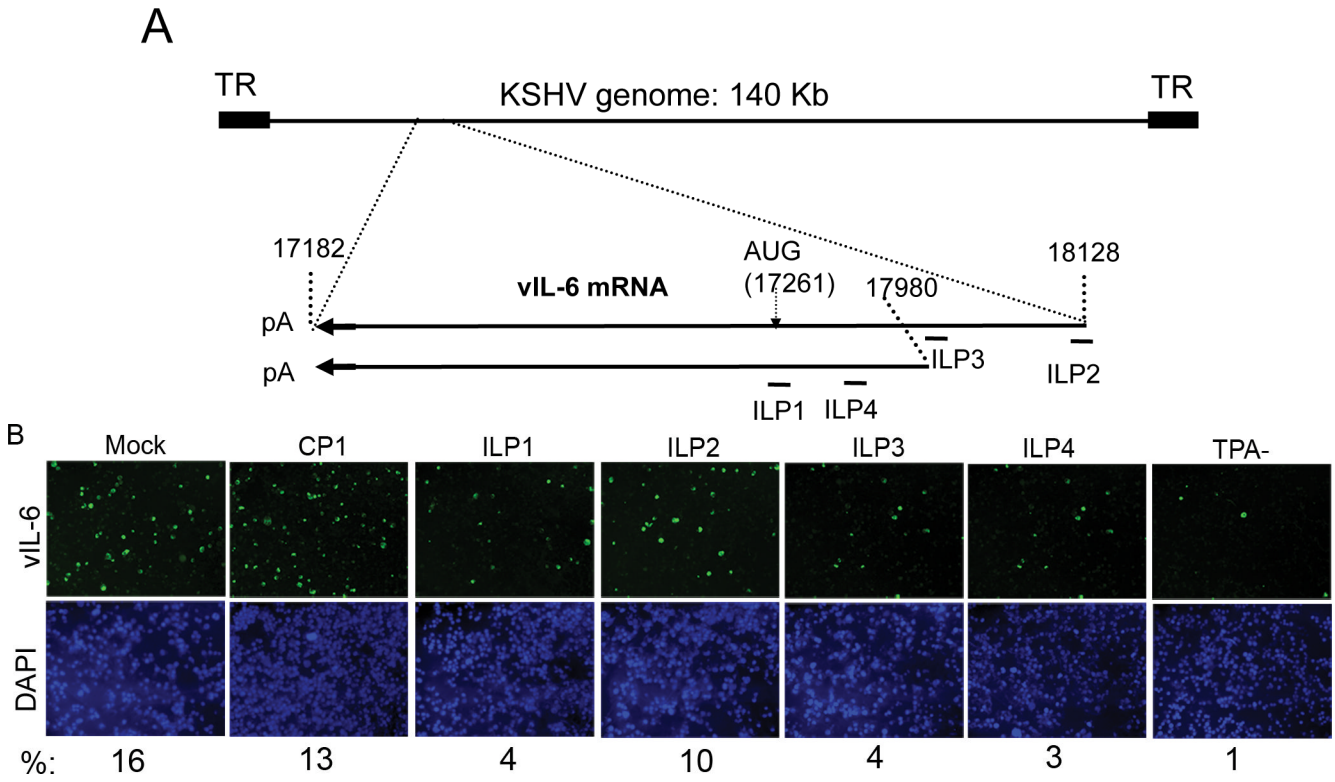

Fig. 1. Schematic of PPMO against vIL-6 and immunofluorescence assay of inhibition

A. Schematic of the KSHV genome, vIL-6 mRNA transcripts and location of PPMO targets. The numbers above the transcript lines indicate nucleotide positions in the KSHV genomic sequence. PPMO ILP1, ILP2, ILP3, and ILP4 are antisense to vIL-6 mRNA and are shown below the transcripts. TR: terminal repeat. The two vIL-6 transcripts have 5'UTRs of differing lengths, but the same coding region and 3' UTR.

B. Inhibition of vIL-6 expression in BCBL-1 cells detected by immunofluorescence assay with rabbit anti-vIL-6 antibody. Cells were treated with ILP1, ILP2, ILP3, ILP4, or CP1 PPMO (16 μM) and induced with TPA, as described in text. The lower image panel was taken with a DAPI filter to reveal all cells. The percentage of vIL-6-positive cells in the samples of the upper panel is reported below the lower panel.

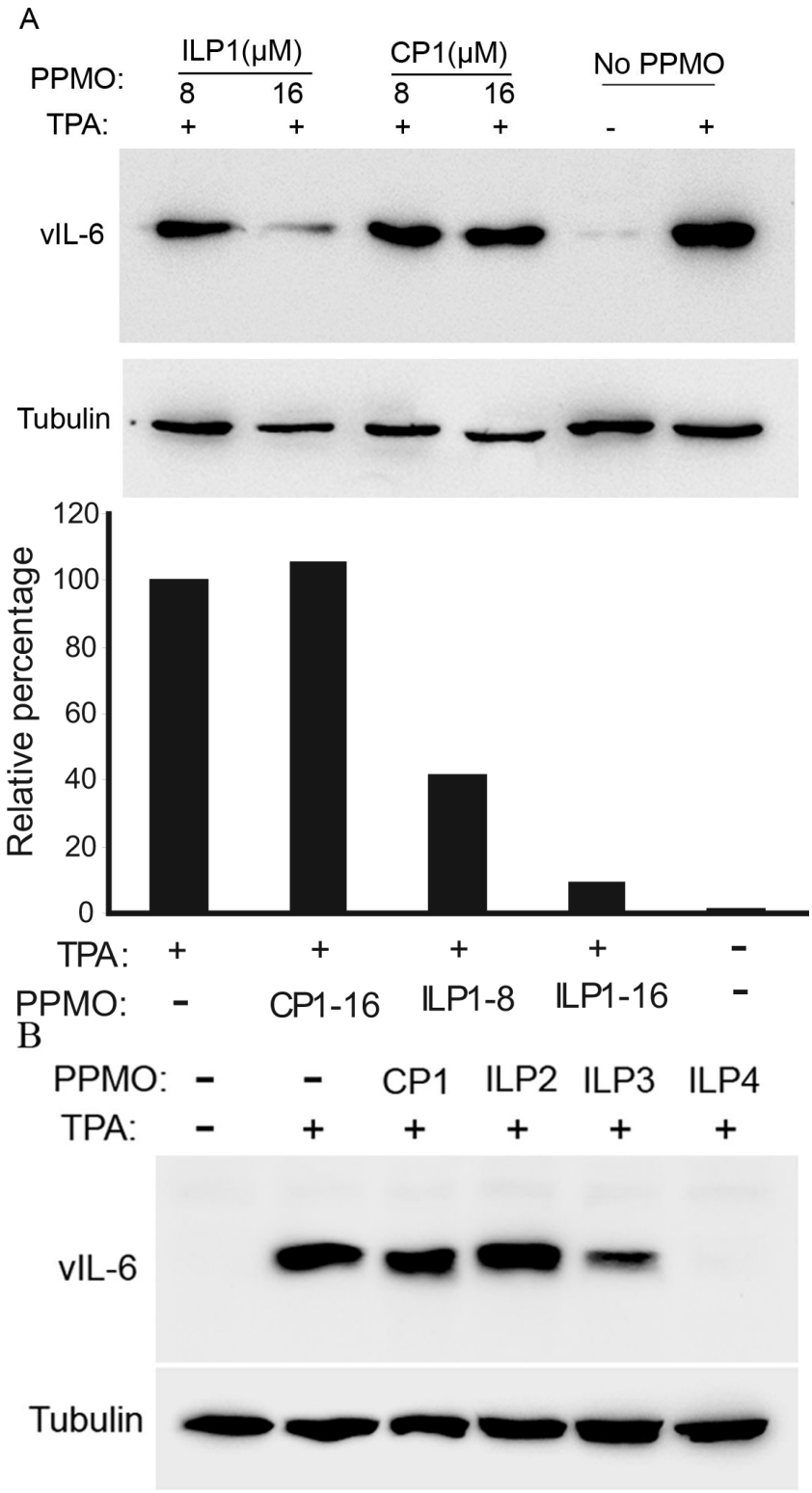

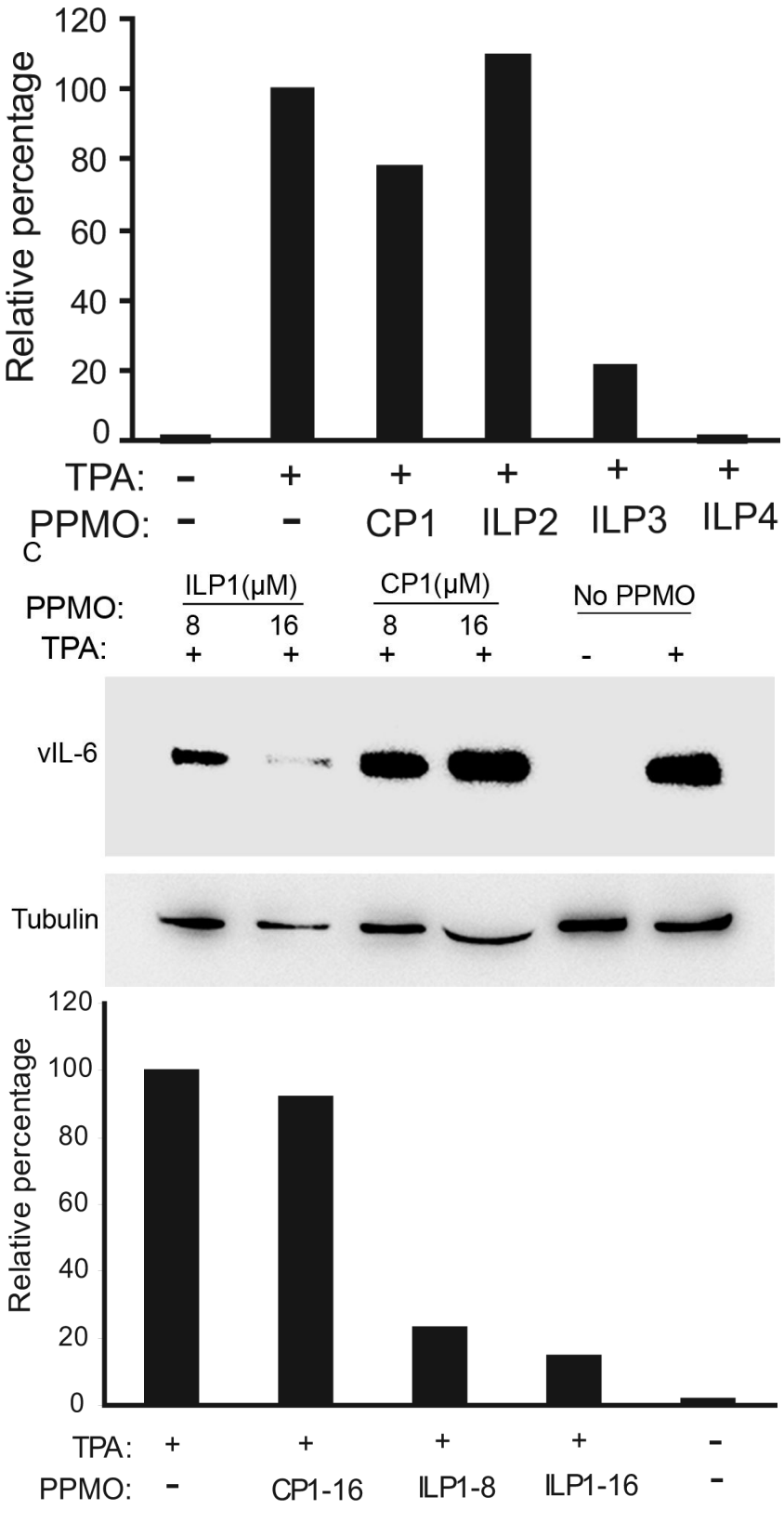

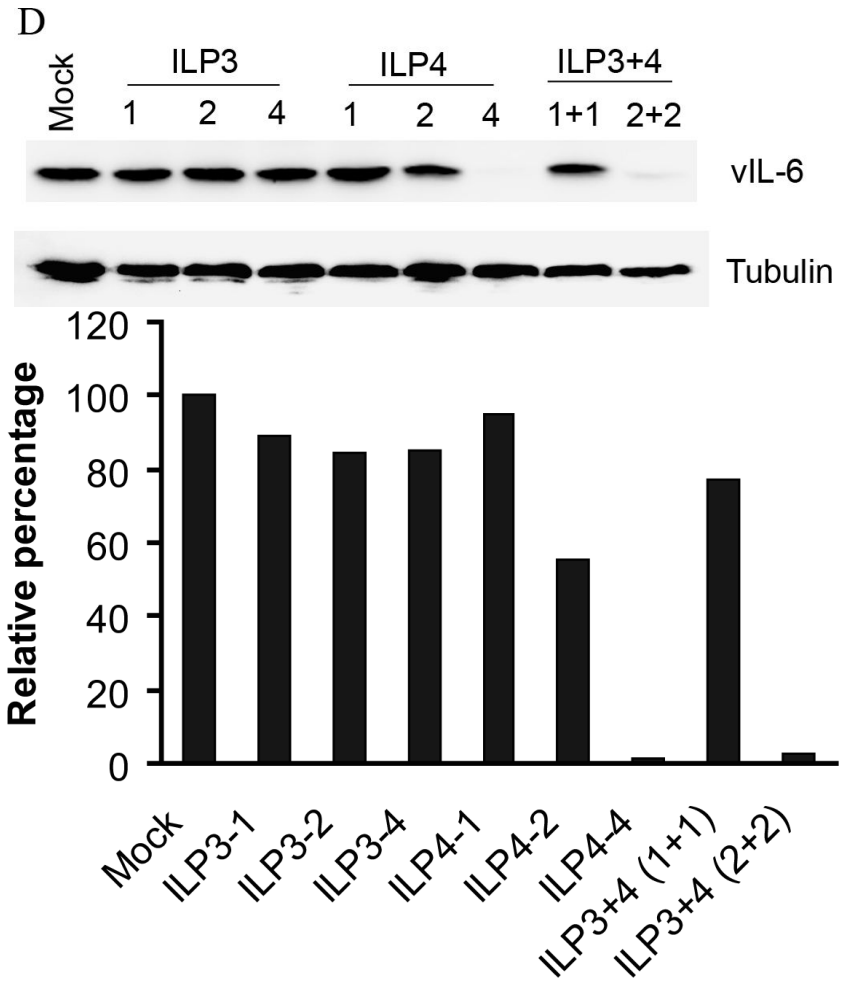

Fig. 2. Suppression of vIL-6 expression in PEL cells by PPMO treatment

A. Western blot analysis of vIL-6 expression in BCBL-1 cells. The same blot was incubated with an anti-β-tubulin antibody as a protein loading control. Mock-treated cells are also included for comparison. Quantitative digital image analysis confirms the dose-responsive inhibition of vIL-6 expression in BCBL-1 cells by ILP1. The vIL-6 expression in cells treated with PPMO is shown as a relative percentage of the mock-treated control.

B. Western blot of BCBL-1 cells treated by PPMO ILP2, ILP3, and ILP4. Quantitative image analysis confirms the inhibition of vIL-6 expression in BCBL-1 cells by ILP3 and ILP4.

C. Suppression of vIL-6 expression in BC-1 cells by PPMO ILP1 treatment. Quantitative image analysis confirms the ILP1-mediated inhibition of vIL-6 expression in BC-1 cells. D. Western blot of BCBL-1 cells after combinatory treatment with ILP3 and ILP4. Quantitative image analysis confirms that inhibition of vIL-6 expression was enhanced when ILP3 and ILP4 were used together.

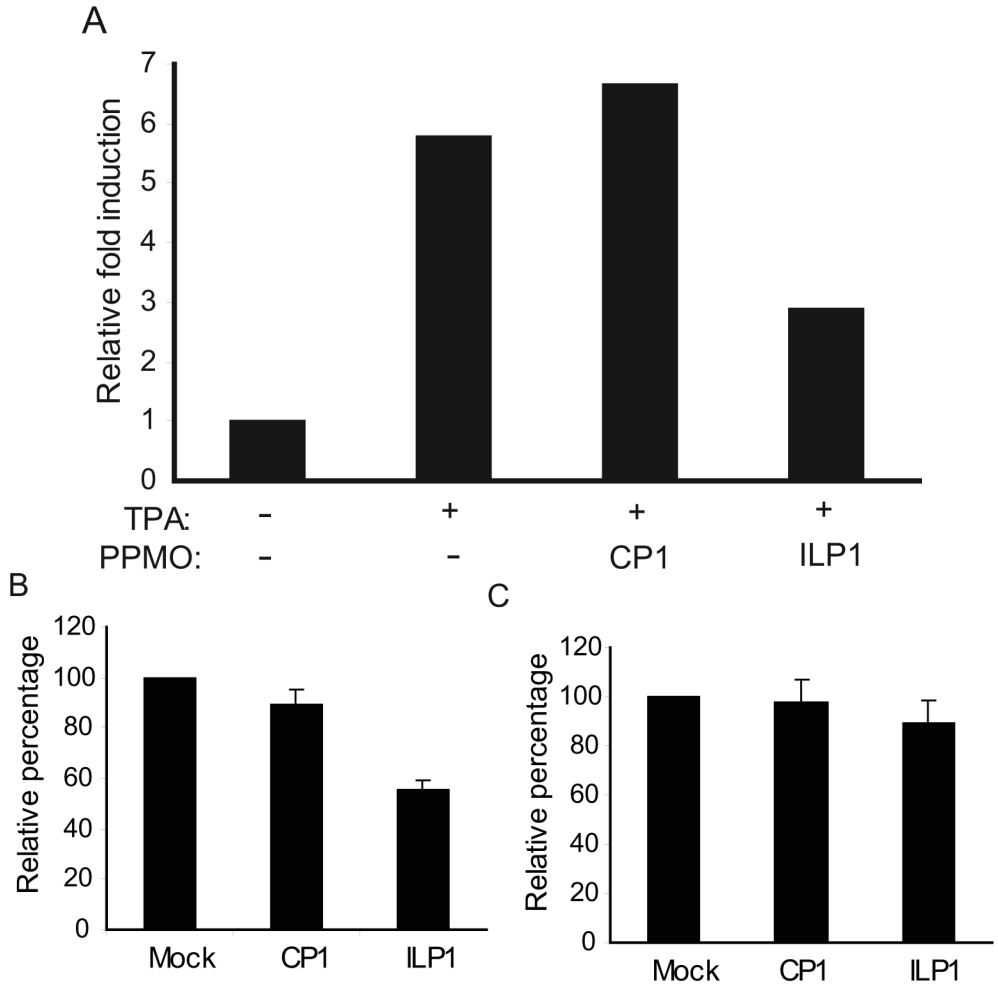

Fig. 3. ILP1 PPMO treatment of BCBL-1 cells reduces hIL-6 expression and cell growth

A. Reduction of hIL-6 expression in BCBL-1 cells after ILP1 treatment. Cells were mock-treated or treated with indicated PPMO, and induced with TPA. Cell culture supernatants were harvested to detect hIL-6 level with EIA. The level of hIL-6 in culture supernatants are expressed as the fold-change relative to the mock treated control. A representative experiment is shown.

B. Reduction of BCBL-1 cell growth after ILP1 treatment. BCBL-1 cells were treated with indicated PPMO and incubated in the absence of TPA. Cells were then assayed for viability. The results are presented as the relative percentage of viable cells as compared to the mock-treated control, which is set as 100%. The average of three tests is shown and the error bar represents variation among the experiments.

C. ILP1 treatment had no effect on BJAB cells. BJAB cells were treated with ILP1 PPMO in a manner similar to that of BCBL-1 cells above. Cell viability assay results are reported as in Fig. 3B.

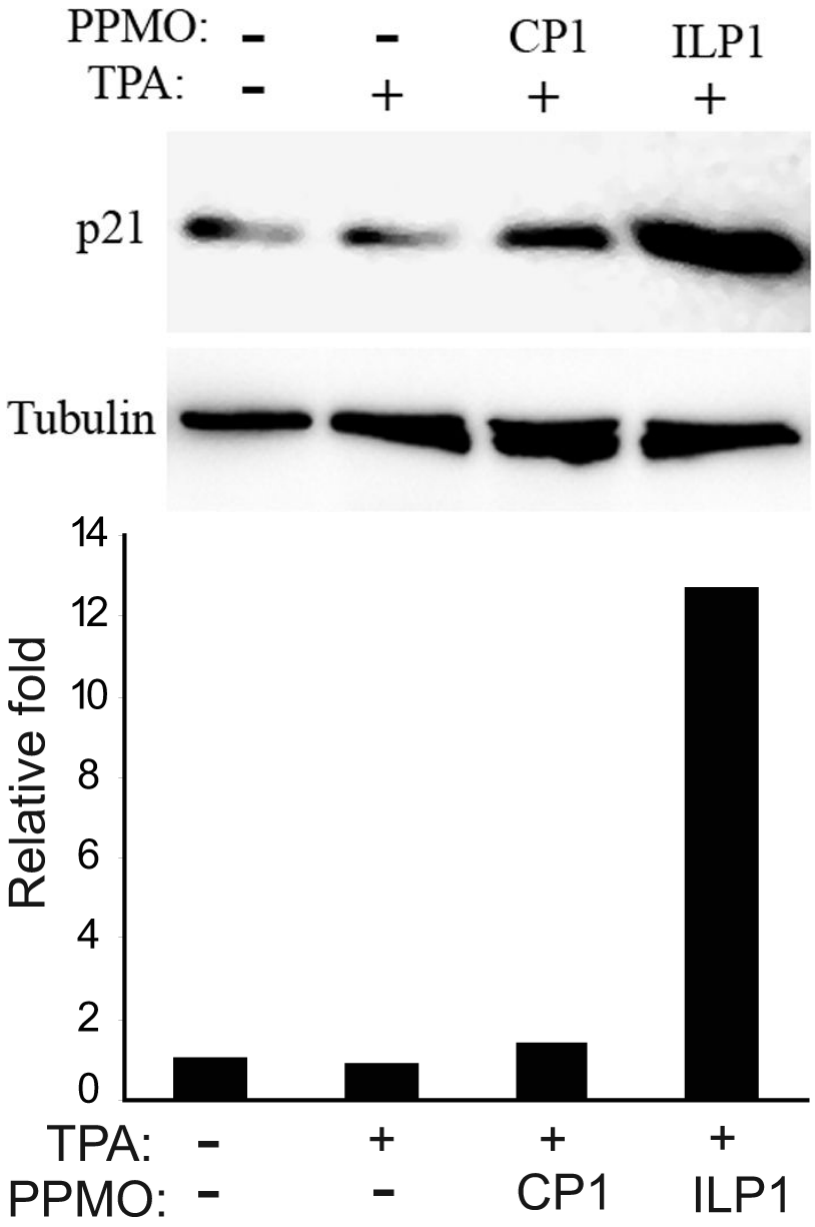

Fig. 4.

Elevation of p21 expression after ILP1 PPMO treatment. Western blot of BCBL-1 cell samples treated as indicated was conducted with p21 antibody. The same blot was stripped and then incubated with an anti-β-tubulin antibody as a protein loading control. A graphic illustration of quantitative image analysis of the blot is shown. The p21 level of each sample is represented as the relative-fold-increase compared to that of the mock-treated control.

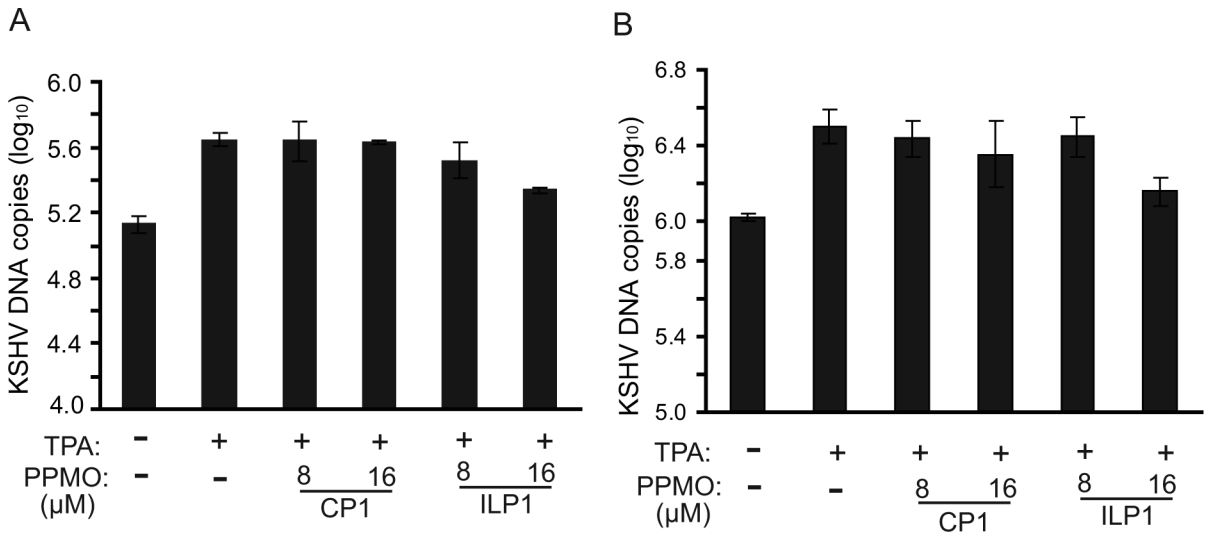

Fig. 5.

Decrease of extra-cellular (A) and cell-associated (B) KSHV DNA level detected by real-time PCR. BCBL-1 cells were treated with PPMO and harvested at 72 h post treatment. DNA was isolated from culture supernatant and from cells. Viral DNA in samples is shown as copies in $\log_{10}$. The average of three experiments is shown and error bars indicate variations of the averages of all three experiments. Real-time PCR was performed with primers from ORF73 and normalized with β–actin, as described in Methods.

Table 1

PPMO sequences and target sites

PPMO	PPMO sequence (5′ to 3′)	Position// relative to start codon of ORF-K2	PPMO target site region
ILP1,*†	GCGGCATACACTAGCCGGTGG	−14 to 7	ORF-K2 translation initiation site
ILP2‡	GAAACACGTCACACGCAAAGTCA	−243 to −219	5′ UTR of vIL-6 mRNA
ILP3‡	ACGCCGTATCCGAACTCTGAGT	−106 to −84	5′ UTR of vIL-6 mRNA
ILP4‡	AGCGGGAGTTACGAAGTCTCAC	−42 to −20	5′ UTR of vIL-6 mRNA
CP1§	GATATACACAACACCCAATT	None	nonsense sequence control

*The underlined nucleotides correspond to the AUG translation initiation codon of vIL-6 mRNA.

†Prepared with the peptide $R_5F_2R_4C$ (P4) conjugated to the PMO at 5′ end.

‡Prepared with the peptide $(RXR)_4XB$ (P7) conjugated to the PMO at 5′ end.

§Two PPMO versions prepared, one conjugated to P4 and the other to P7.

//GenBank accession number for the KSHV genome sequence is U75698. The position numbers indicate PPMO target sites relative to the ORF-K2 AUG translation initiation codon in vIL-6 mRNA.